




Article

Synthesis of a Novel Hydrazone of Thieno[2,3-*d*]pyrimidine Clubbed with Ninhydrin: X-ray Crystal Structure and Computational Investigations

Mezna Saleh Altowyan ¹, Matti Haukka ², Saied M. Soliman ³, Assem Barakat ^{4,*}, Ahmed T. A. Boraie ^{5,*} and Manar Sopaih ⁵

¹ Department of Chemistry, College of Science, Princess Nourah bint Abdulrahman University, P.O. Box 84428, Riyadh 11671, Saudi Arabia

² Department of Chemistry, University of Jyväskylä, P.O. Box 35, FI-40014 Jyväskylä, Finland

³ Chemistry Department, Faculty of Science, Alexandria University, P.O. Box 426, Alexandria 21321, Egypt

⁴ Department of Chemistry, College of Science, King Saud University, P.O. Box 2455, Riyadh 11451, Saudi Arabia

⁵ Chemistry Department, Faculty of Science, Suez Canal University, Ismailia 41522, Egypt

* Correspondence: ambarakat@ksu.edu.sa (A.B.); ahmed_tawfeek83@yahoo.com or ahmed_boraie@science.suez.edu.eg (A.T.A.B.); Tel.: +966-11467-5901 (A.B.); Fax: +966-11467-5992 (A.B.)

Abstract: The novel hydrazone-containing thieno[2,3-*d*]pyrimidine, namely, *N'*-(1,3-dioxo-1,3-dihydro-2*H*-inden-2-ylidene)-2-(4-oxo-5,6,7,8-tetrahydrobenzo[4,5]thieno[2,3-*d*]pyrimidin-3(4*H*)-yl)acetohydrazide **4** was synthesized in a very good yield from the reaction of the triketoester **1** or ninhydrin **2** with the exocyclic acetohydrazide **3** in methanol. Good-quality crystals of **4** were obtained by recrystallization of the compound from the DMF/MeOH solvent mixture. The target product **4** crystallized in the triclinic crystal system and *P*-1 space group. The topology analysis of molecular packing indicated that the H ... H (30.4%), O ... H (22.0%) and H ... C (17.0%) contacts are the most dominant intermolecular interactions in the crystal of **4**, while the O ... H, N ... H, H ... C, N ... C, O ... C, C ... C and O ... O are the only contacts which have shorter interaction distances than the vdWs radii sum of the interacting atoms. The structure of **4** is optimized and the calculated structure showed good agreement with the experimental one. Additionally, MEP, HOMO, LUMO and the reactivity descriptors were calculated.

Keywords: thieno[2,3-*d*]pyrimidine; ninhydrin; hydrazone; X-ray crystal structure; Hirshfeld



Citation: Altowyan, M.S.; Haukka, M.; Soliman, S.M.; Barakat, A.; Boraie, A.T.A.; Sopaih, M. Synthesis of a Novel Hydrazone of Thieno[2,3-*d*]pyrimidine Clubbed with Ninhydrin: X-ray Crystal Structure and Computational Investigations. *Crystals* **2023**, *13*, 384. <https://doi.org/10.3390/cryst13030384>

Academic Editor: Kil Sik Min

Received: 22 January 2023

Revised: 19 February 2023

Accepted: 21 February 2023

Published: 23 February 2023



Copyright: © 2023 by the authors. Licensee MDPI, Basel, Switzerland. This article is an open access article distributed under the terms and conditions of the Creative Commons Attribution (CC BY) license (<https://creativecommons.org/licenses/by/4.0/>).

1. Introduction

Thieno[2,3-*d*]pyrimidines are unique fused privilege structures which have shown a high degree of applications in several fields such as agriculture, bioorganic chemistry and medicinal chemistry [1]. Thieno[2,3-*d*]pyrimidines are the bioisosteres of the purine scaffold, which play a crucial role in many physiological functions such as cell proliferation and respiration; thus, the synthesis of a new analogues-based purine core structures, such as thieno[2,3-*d*]pyrimidines, for the purpose of drug discovery development is of interest. Many thieno[2,3-*d*]pyrimidines are found in the structure of VEGFR [2,3], tyrosine kinases [4] and phosphodiesterase inhibitors [5] which are important biological compounds that occur in the human body [6]. In recent decades, many of thieno[2,3-*d*]pyrimidines have been designed, synthesized and identified as anti-inflammatory [7], antipyretic [8], analgesic [9], antimicrobial [10] radioprotective [11], antihistaminic [12] and anticancer [13] agents. Additionally, thienopyrimidines have medicinal applications [14] against diseases such as tuberculosis, cerebral ischemia, malaria, Parkinson's and Alzheimer's [14,15].

Recently, Gad et al. [16] designed and synthesized new thieno[2,3-*d*]pyrimidine analogues as anticancer drug candidates that displayed promising efficacy on breast cancer. The Khaled A. M. Abouzid research group discovered a new chemical entity based on

thieno[2,3-*d*]pyrimidines and was identified as an anticancer agent targeted therapy for PI3K enzyme inhibition [17].

In fact, ninhydrin is a triketone analogue which has unique chemical properties and is used as a building block for many organic transformations. Additionally, ninhydrin is widely employed as a fluorescence agent for the detection of latent fingerprints in forensic science [18–20] as well as in other fields such chemiluminescence [21] or for the development of new fluorophore systems [22]. Ninhydrin is derived from the indanone core structure, which exists in many natural products. Interestingly, it displays biological potency such as anti-inflammatory, anti-tumor, anti-allergy, free radical scavenger, and antimicrobial activities [23,24]. Therefore, combining two important pharmacophores such as the thieno[2,3-*d*]pyrimidine moiety and the ninhydrin group is of interest and may lead to the discovery of a new privileged and lead structure for further research.

It is well known that hydrazone is a big class of organic compounds that showed high importance in the pharmaceutical field, as this functional group was identified as a core structure for coordination chemistry. Additionally, their metal complexes were reported to have many biological applications as anti-fungal and anti-microbial agents, and they also have interesting catalytic applications [25,26].

According to these findings and in continuation with our research program [15,27], we report herein the synthesis of a new organic material based on thieno[2,3-*d*]pyrimidines clubbed with a ninhydrin scaffold linked with hydrazone. The structure aspects were elucidated by X-ray single crystal structure technique combined with Hirshfeld and DFT calculations.

2. Materials and Methods

2.1. General

All chemicals and solvents used in this study were purchased from Sigma Aldrich or El Nasr Company for Intermediate Chemicals with at least 98% purity and used without further purification. Melting points were measured via a melting-point apparatus (SMP10) in an open capillary and are uncorrected. Nuclear magnetic resonance (^1H -NMR and ^{13}C -NMR) spectra were determined in DMSO- d_6 on a Bruker AC 400 MHz and a Bruker AC 100 MHz spectrometer, respectively, where tetramethylsilane was used as internal standard. Chemical shifts were described in δ (ppm), and coupling constants are given in Hz. Elemental analysis (CHNS) was performed on a Flash EA-1112 instrument.

2.2. Synthesis of *N'*-(1,3-dioxo-1,3-dihydro-2H-inden-2-ylidene)-2-(4-oxo-5,6,7,8-tetrahydrobenzo[4,5]thieno[2,3-*d*]pyrimidin-3(4H)-yl)Acetohydrazide **4**

The synthesis of **4** was performed from the two precursors **1** and **2** as follows:

A mixture of triketoester **1** (0.352 g, 1.0 mmol) or ninhydrin **2** (0.178 g, 1.0 mmol) and hydrazide **3** (0.278 g, 1.0 mmol) was refluxed in MeOH 10 mL for 4 h, the formed precipitates were filtered off, dried under vacuum and recrystallized from DMF/MeOH.

Yield: 0.328 g, 78 % (from **1**), 0.311 g, 74 % (from **2**), as shiny yellow crystals (DMF/MeOH). M.p. 259–260 °C; ^1H -NMR (400 MHz, DMSO- d_6) δ 12.61 (s, 1H), 8.37 (s, 1H), 8.34–7.94 (m, 4H), 5.29 (s, 2H), 2.90–2.74 (m, 4H), 1.82–1.78 (m, 4H); ^{13}C NMR (100 MHz, DMSO- d_6) δ 162.26 (2C), 157.28 (2C), 148.35 (CH), 141.94 (2C), 140.23 (C), 137.21 (CH), 137.04 (CH), 133.85 (2C), 131.28 (C), 124.33 (CH), 123.90 (CH), 122.09 (C), 40.43, (NCH₂), 25.74 (CH₂), 25.01 (CH₂), 22.85 (CH₂), 22.20 (CH₂); Elemental analysis (CHNS) calculated for [C₂₁H₁₆N₄O₄S]: C, 59.99; H, 3.84; N, 13.33; S, 7.63 found C, 60.08; H, 3.81; N, 13.23; S, 7.69.

2.3. X-ray Structure Determination

The crystal structure of **4** was solved using X-ray diffraction data according the method described in Supplementary data [28–31]. The crystallographic details are summarized in Table 1.

Table 1. Crystal data and structure refinements for **4**.

	4
CCDC	2237068
empirical formula	C ₂₁ H ₁₆ N ₄ O ₄ S
fw	420.44
temp (K)	120(2) K
λ (Å)	1.54184
cryst syst	Triclinic
space group	P 1
<i>a</i> (Å)	5.5257 (2)
<i>b</i> (Å)	10.9956 (5)
<i>c</i> (Å)	15.4836 (6)
α (°)	95.881(3)
β (deg)	100.164(3)
γ (°)	92.139(3)
<i>V</i> (Å ³)	919.65 (7)
<i>Z</i>	2
ρ_{calc} (Mg/m ³)	1.518
μ (Mo K α) (mm ^{−1})	1.909
No. reflections	18314
Unique reflections	3813
Completeness to $\theta = 67.684^\circ$	99.9%
GOOF (<i>F</i> ²)	1.029
<i>R</i> _{int}	0.0688
<i>R</i> ₁ ^a (<i>I</i> ≥ 2 σ)	0.0479
<i>wR</i> ₂ ^b (<i>I</i> ≥ 2 σ)	0.1212

$$^a R_1 = \sum ||F_o| - |F_c|| / \sum |F_o|, \quad ^b wR_2 = \{\sum [w(F_o^2 - F_c^2)^2] / \sum [w(F_o^2)^2]\}^{1/2}.$$

2.4. Hirshfeld Surface Analysis

The topology analyses were performed using Crystal Explorer 17.5 program [32].

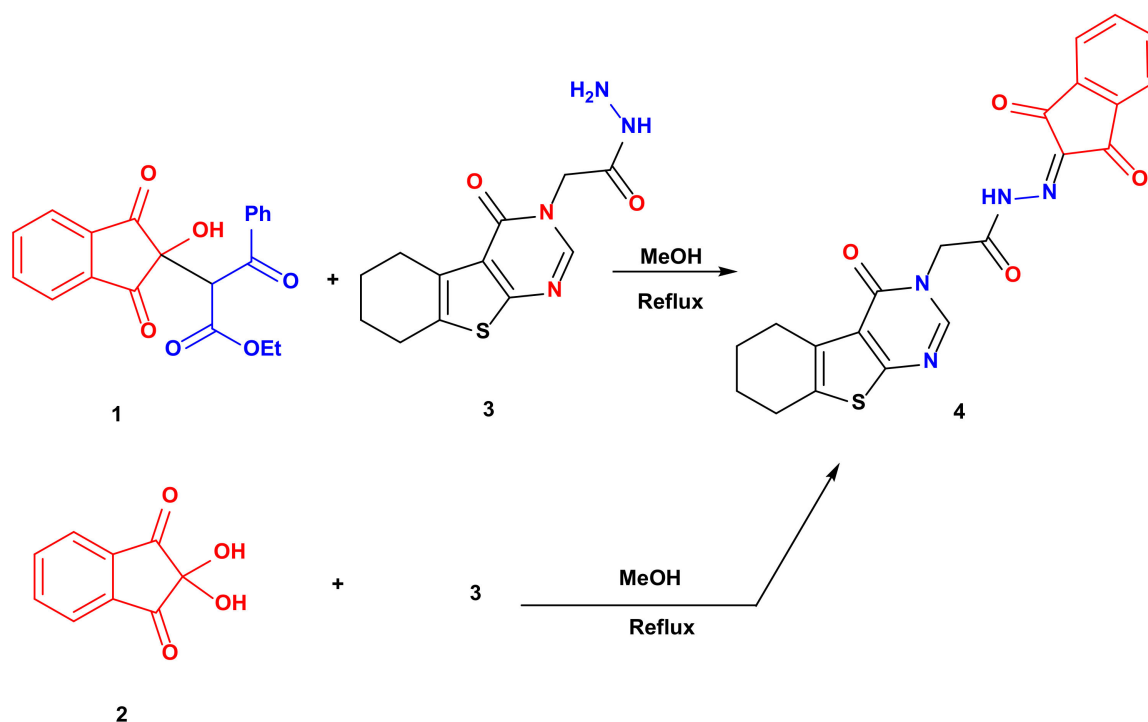
3. Computational Methods

DFT calculations were performed for a single molecule in a vacuum, without solvation or cluster models, using Gaussian 09 software package [33,34] utilizing B3LYP/6-31G(d,p) level of theory. Natural bond orbital analyses were performed using NBO 3.1 program [35].

4. Results and Discussion

4.1. Synthesis and NMR Characterizations of **4**

Refluxing ethyl 2-(2-hydroxy-1,3-dioxo-2,3-dihydro-1*H*-inden-2-yl)-3-oxo-3-phenylpropanoate **1** or ninhydrin **2** with 2-(4-oxo-5,6,7,8-tetrahydrobenzo[4,5]thieno[2,3-*d*]pyrimidin-3(4*H*)-yl)acetohydrazide **3** in methanol for 4 h afforded *N*'-(1,3-dioxo-1,3-dihydro-2*H*-inden-2-ylidene)-2-(4-oxo-5,6,7,8-tetrahydrobenzo[4,5]thieno[2,3-*d*]pyrimidin-3(4*H*)-yl)acetohydrazide **4** in a very good yield (78 and 74% yields, respectively) (Scheme 1). The ¹H NMR spectrum revealed significant signals confirming the product formation such as the NH proton at 12.61 ppm, pyrimidine proton at 8.37 ppm and the methylene protons attached to nitrogen at 5.29 ppm. Moreover, the ¹³C NMR spectrum showed the carbonyl carbons at 162.26 and 157.28 ppm.



Scheme 1. Synthesis of 4.

4.2. Crystal Structure Description

A single crystal of 4 was examined using X-ray diffraction, and the resulting structure is presented in Figure 1, which agrees very well with its spectral characterizations, confirming the successful trial to synthesize the target compound. The structure of 4 crystallized in the triclinic crystal system and P-1 space group with lattice parameters of $a = 5.5257$ (2) Å, $b = 10.9956$ (5) Å, $c = 15.4836$ (6) Å, $\alpha = 95.881$ (3)°, $\beta = 100.164$ (3)°, $\gamma = 92.139$ (3)° and unit cell volume of 919.65 (7) Å³, and two molecules per unit cell (Table 1). Selected bond distances and angles are given in Table 2. The structure of 4 is stabilized by short intramolecular N(3)-H(3)...O(3) hydrogen bond with donor–acceptor distance of 2.847 (2) Å. The inter- and intra-molecular N-H...O hydrogen bond contacts are presented in Figure 2.

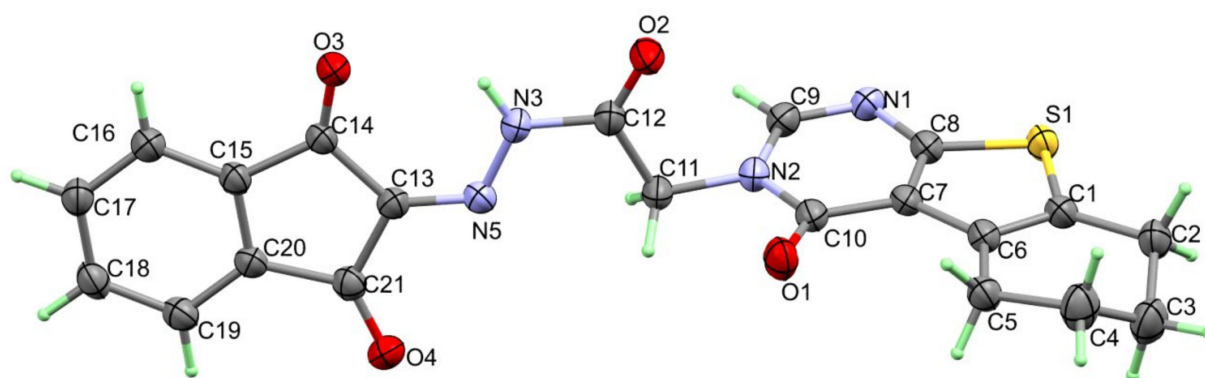
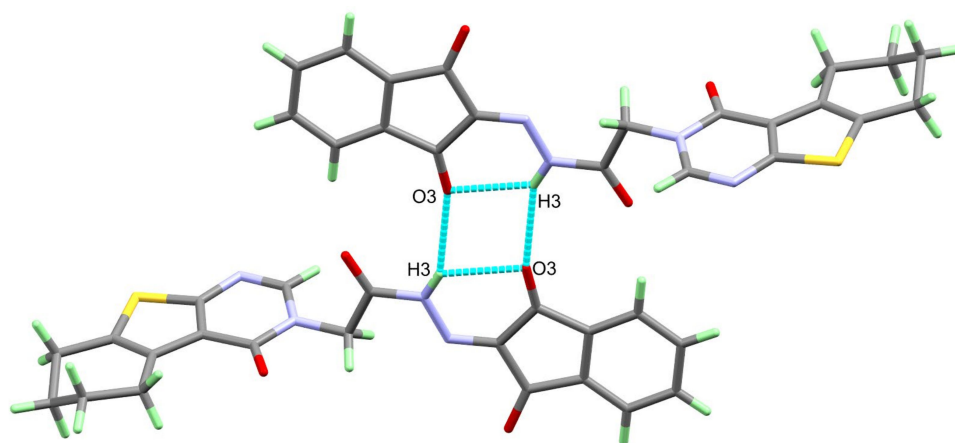


Figure 1. X-ray structure of 4.

Table 2. Bond lengths (Å) and angles (°) for **4**.

Bond	Length/Å	Bond	Length/Å
S(1)-C(8)	1.731 (2)	N(1)-C(8)	1.362 (3)
S(1)-C(1)	1.741 (2)	N(2)-C(9)	1.365 (3)
O(1)-C(10)	1.222 (3)	N(2)-C(10)	1.410 (3)
O(2)-C(12)	1.206 (3)	N(2)-C(11)	1.460 (3)
O(3)-C(14)	1.216 (3)	N(3)-N(5)	1.341 (3)
O(4)-C(21)	1.215 (3)	N(3)-C(12)	1.393 (3)
N(1)-C(9)	1.300 (3)	N(5)-C(13)	1.292 (3)
Bonds	Angle/°	Bonds	Angle/°
C(8)-S(1)-C(1)	91.18 (11)	C(13)-N(5)-N(3)	119.38 (19)
C(9)-N(1)-C(8)	114.0 (2)	C(6)-C(1)-C(2)	125.2 (2)
C(9)-N(2)-C(10)	123.85 (19)	C(6)-C(1)-S(1)	112.99 (17)
C(9)-N(2)-C(11)	118.31 (19)	C(2)-C(1)-S(1)	121.78 (18)
C(10)-N(2)-C(11)	117.8 (2)	C(1)-C(2)-C(3)	109.1 (2)
N(5)-N(3)-C(12)	117.50 (19)		

**Figure 2.** Hydrogen bond dimer of **4**.

On the other hand, the analysis of the hydrogen bonding interactions in **4** revealed the presence of short intermolecular N(3)-H(3)...O(3) hydrogen bonds, which play an important role in the molecular packing of the studied system (Figure 2). The N(3)...O(3) donor–acceptor distance is 3.129 (3) Å, and the symmetry code of the hydrogen bond acceptor is $-x + 1, -y, -z + 1$ (Table 3).

Table 3. Hydrogen bond parameters (Å and °) for **4**.

D-H ... A	D-H	H ... A	D ... A	D-H ... A
N(3)-H(3)...O(3)	0.85 (3)	2.24 (3)	2.847 (2)	128 (3)
N(3)-H(3)...O(3) ¹	0.85 (3)	2.35 (3)	3.129 (3)	154 (3)

Symmetry Code. ¹ $1-x+1, -y, -z+1$.

4.3. Hirshfeld Analysis

The decomposition of the different intermolecular contacts controlling the molecular packing of **4** was performed using Hirshfeld calculations. The decomposed fingerprint plots shown in Figure 3 gave a quantitative summary of each intermolecular contact occurring in the crystal. It is quite clear that there are large number of contacts which control the packing of the different molecular units in the crystal, where the H ... H (30.4%), O ... H (22.0%) and H ... C (17.0%) contacts are the most dominant. In addition, there are some contributions from the N ... H (7.1%), O ... C (6.5%), S ... H (5.1%) and S ... C (4.4%) contacts (Figure 4). Not all contacts presented in Figure 2 have the characteristic feature

of short interactions, where the O ... H, N ... H, H ... C, N ... C, O ... C, C ... C and O ... O are the only contacts which appear as red spots in Figure 5. These short distance contacts and their corresponding distances are collected in Table 4. The majority of these short interactions have the characteristic sharp peaks in the fingerprint plot (Figure 3). Additionally, the results revealed the presence of significant amount of short N ... C and C ... C contacts which gave an indication on the presence of some π - π stacking interactions. The shape index and curvedness maps did not give any good indication about this type of interaction, probably due to the incomplete stacking of the aromatic π -system among the molecular units.

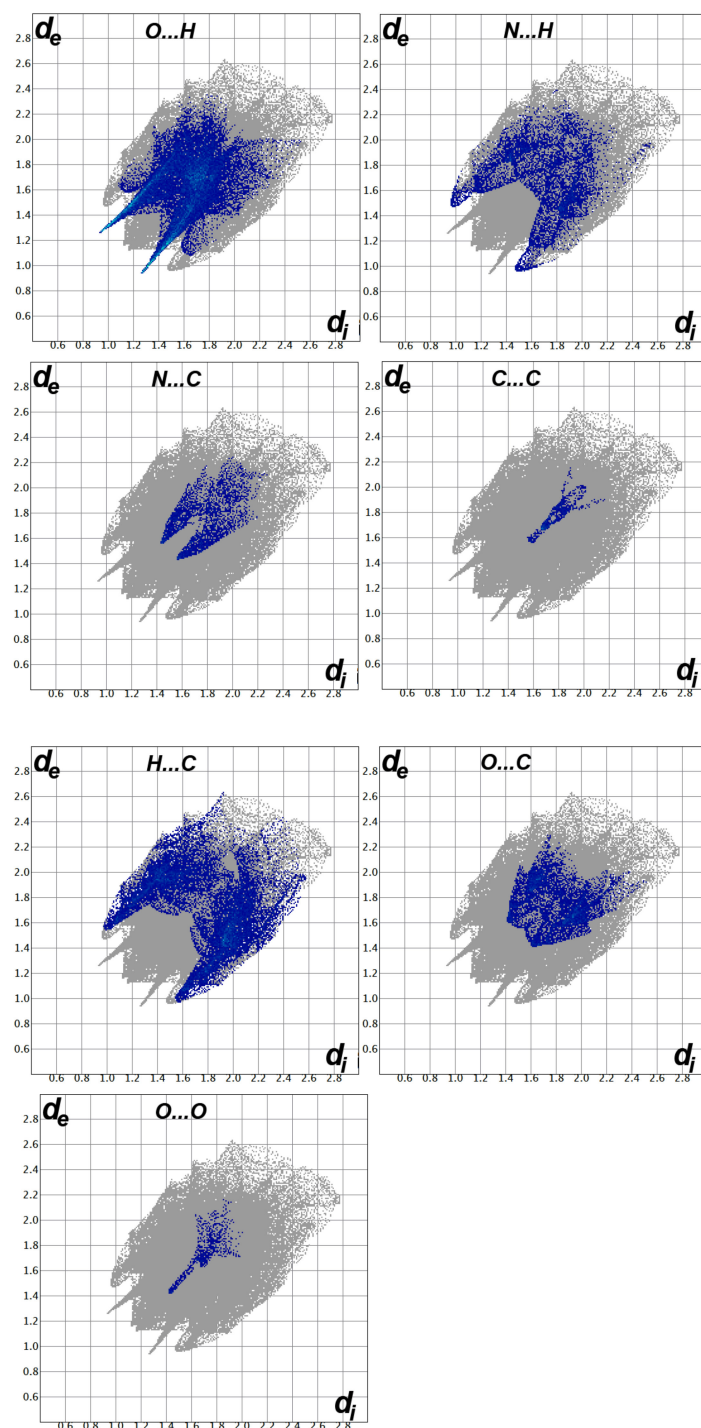


Figure 3. Decomposed fingerprint plots for the important interactions in 4.

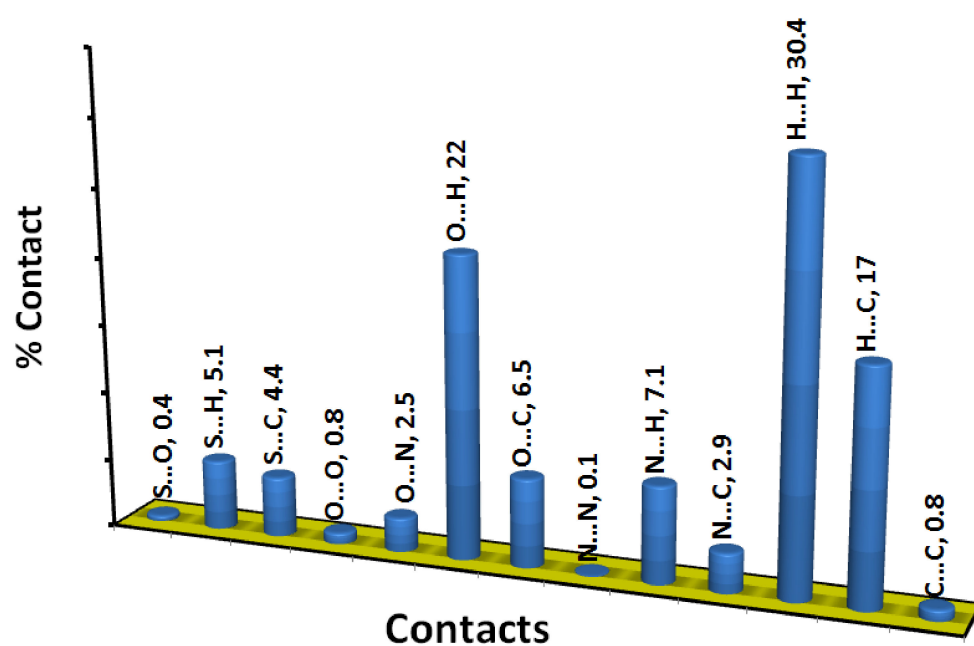


Figure 4. All intermolecular interactions and their percentages.

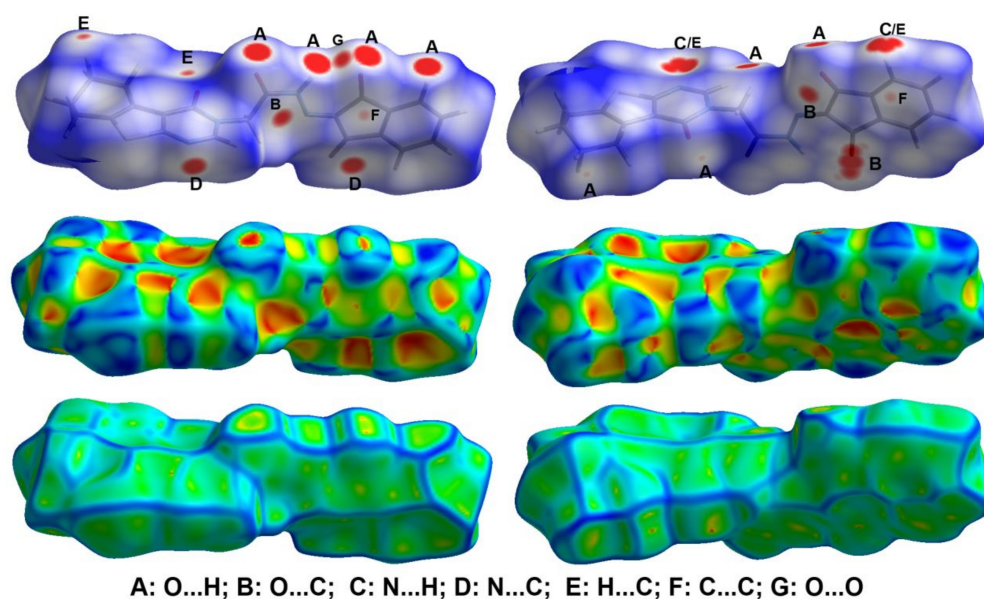


Figure 5. Hirshfeld surfaces of 4.

Table 4. All short contacts and their interaction distances.

Contact	Distance	Contact	Distance
O3 ... C14	3.043	O1 ... H4B	2.556
O3 ... C15	3.18	O4 ... H11B	2.303
O4 ... C12	3.028	O2 ... H16	2.215
N1 ... C21	2.999	O3 ... H3	2.203
N1 ... H19	2.446	C14 ... C19	3.337
H19 ... C8	2.621	O3 ... O3	2.853
H19 ... C9	2.542		
H4A ... C10	2.669		

4.4. DFT Studies

The optimized structure of **4** using B3LYP/6-31G(d,p) level of theory [36–38] is shown in Figure 6 along with its overlay with the experimental one. The optimized structure gave no any imaginary frequencies indicating real energy minimum structure. There are some expected deviations in the calculated bond distances and angles (Figures S1 and S2, Table S1, Supplementary data). These deviations are generally attributed to the difference in the physical state between them, where the calculated structure is for a single molecule while the experimental structure is in the solid state. The former is free from the environment effects, while in the latter, the presence of intermolecular forces among molecular units has a great impact on the geometric parameters. Generally, there are good straight-line correlations, as shown in Figure 7, between the calculated and experimental geometric parameters ($R^2 = 0.9963$ – 0.9829).

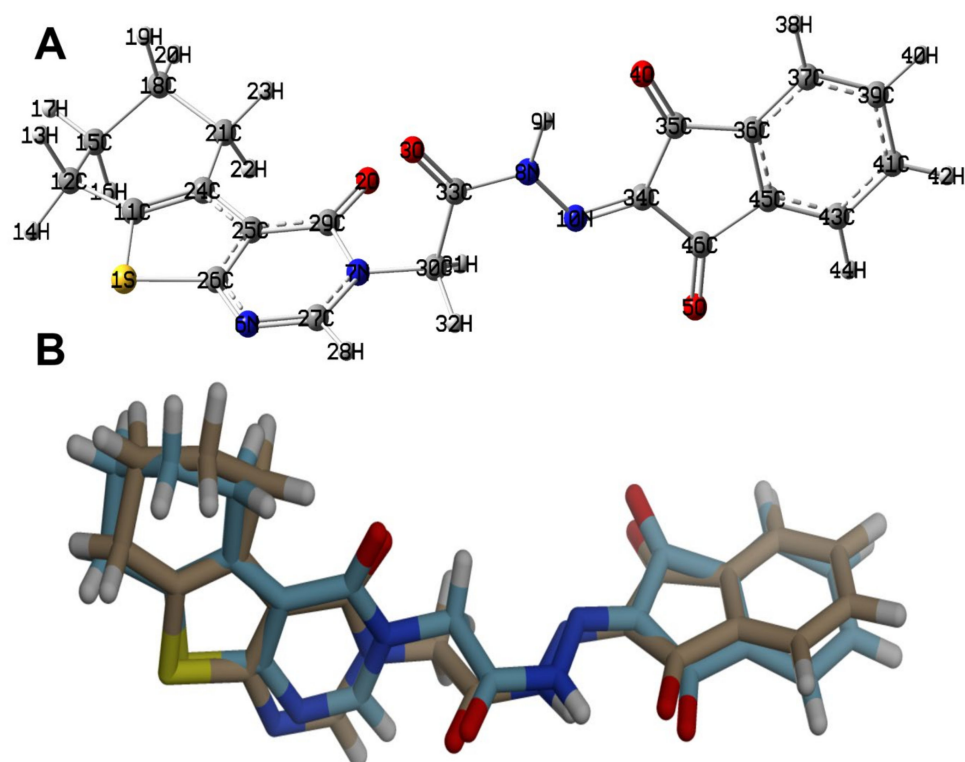


Figure 6. The calculated structure (A) and its overlay with the X-ray structure (B).

The charges based on NBO calculations were calculated and are presented in Figure 8. The distribution of the charges at the atomic sites has a great impact on the electronic properties such as dipole moment. It is clear from Figure 8 that the S-atom has high electropositive nature (0.4699 e). Additionally, all H- and C-atoms bonded to O or N sites have positive natural charges. In contrast, the rest of the carbon atoms as well as the N and O sites are electronegative. As an outcome of this charge distribution, the compound has a high polar nature (5.5906 Debye). The dipole moment vector is overlaid on the molecular electrostatic potential (MEP), as shown in Figure 9.

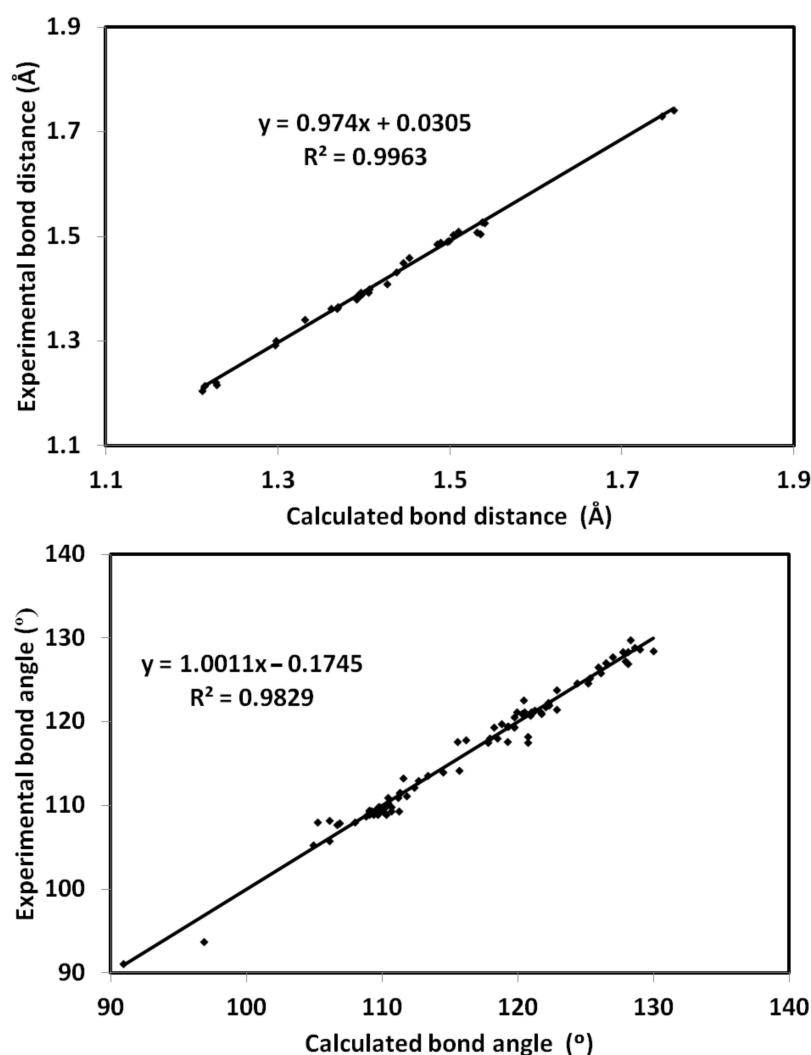


Figure 7. Correlations between X-ray geometric parameters and calculated data.

In MEP, the most electronegative red regions are close to the carbonyl carbon. In contrast, the blue electropositive regions are close to the hydrogen sites (Figure 9). In the same figure, the HOMO and LUMO presentations are also explored. It is clear that the HOMO and LUMO levels are mainly located over the π -system of the studied molecule. The one electron excitation from HOMO to LUMO could be described as an intramolecular charge transfer from the two fused aromatic rings in the tricyclic system to the ninhydrin moiety. The energy of this electronic transition is 2.5603 eV.

Additionally, the HOMO (−5.6777 eV) and LUMO (−3.1147 eV) energies were used to calculate the ionization potential ($I = -E_{\text{HOMO}}$), electron affinity ($A = -E_{\text{LUMO}}$), chemical potential ($\mu = -(I + A)/2$), hardness ($\eta = (I - A)/2$) as well as electrophilicity index ($\omega = \mu^2/2\eta$) [39–45]. Their values were calculated to be 5.6777, 3.1147, −4.3795, 2.5603 and 3.7765 eV, respectively. The calculated parameters have important rule in the biomolecular reactivity.

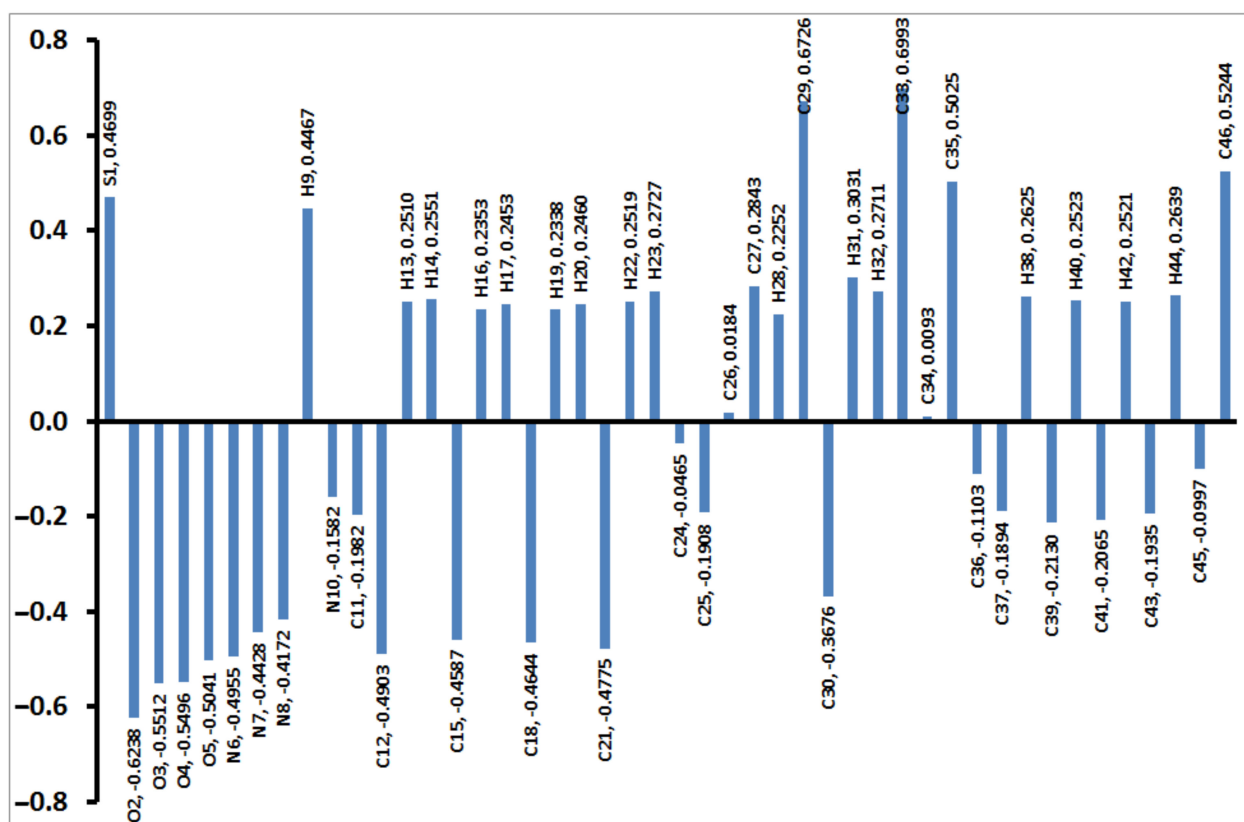


Figure 8. Natural atomic charges of 4.

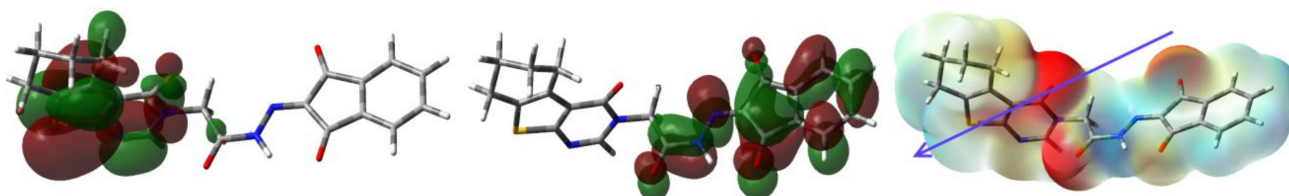


Figure 9. The MEP, HOMO and LUMO of 4.

4.5. Natural Orbital Analysis

In the light of the importance of electron delocalization (ED) via conjugation effect on the stability of molecular system, the different electron delocalization processes in **4** were calculated [46,47]. The $\sigma\text{-}\sigma^*$, $\pi\text{-}\pi^*$, $n\text{-}\sigma^*$ and $n\text{-}\pi^*$ ED and their stabilization energies ($E^{(2)}$) are listed in Table 5. The maximum stabilization energies are 5.12, 27.20, 30.89 and 53.25 kcal/mol for the $\text{BD}(1)\text{C34-C46}\rightarrow\text{BD}\times(1)\text{N8-N10}$, $\text{BD}(2)\text{C25-C26}\rightarrow\text{BD}\times(2)\text{O2-C29}$, $\text{LP}(2)\text{O2}\rightarrow\text{BD}\times(1)\text{N7-C29}$ and $\text{LP}(1)\text{N7}\rightarrow\text{BD}\times(2)\text{N6-C27}$ ED processes, respectively.

Table 5. Donor (NBO_i)–acceptor (NBO_j) interactions in **4**^a.

NBO _i	NBO _j	E ⁽²⁾	NBO _i	NBO _j	E ⁽²⁾
BD(1)C34–C46	BD×(1)N8–N10	5.12	LP(2)O2	BD×(1)N7–C29	30.89
BD(2)O4–C35	BD×(2)N10–C34	5.69	LP(2)O2	BD×(1)C25–C29	17.44
BD(2)O 5–C46	BD×(2)N10–C34	5.24	LP(2)O3	BD×(1)N 8–C33	28.04
BD(2)N 6–C27	BD×(2)C25–C26	19.23	LP(2)O3	BD×(1)C30–C33	22.7
BD(2)N10–C34	BD×(2)O4–C35	15.23	LP(2)O4	BD×(1)C34–C35	18.69
BD(2)N10–C34	BD×(2)O5–C46	14.14	LP(2)O4	BD×(1)C35–C36	20.53
BD(2)C11–C24	BD×(2)C25–C26	14.19	LP(2)O5	BD×(1)C34–C46	23.52
BD(2)C25–C26	BD×(2)O2–C29	27.20	LP(2)O5	BD×(1)C45–C46	21.77
BD(2)C25–C26	BD×(2)N6–C27	12.61	LP(1)N6	BD×(1)N7–C27	14.9
BD(2)C25–C26	BD×(2)C11–C24	16.05	LP(1)N6	BD×(1)C25–C26	9.67
BD(2)C36–C37	BD×(2)O 4–C35	19.79	LP(1)N7	BD×(1)C30–C33	7.26
BD(2)C36–C37	BD×(2)C39–C41	19.37	LP(1)N10	BD×(1)C34–C35	12.11
BD(2)C36–C37	BD×(2)C43–C45	19.79	LP(2)S1	BD×(2)C11–C24	19.16
BD(2)C39–C41	BD×(2)C43–C45	19.23	LP(2)S1	BD×(2)C25–C26	22.9
BD(2)C39–C41	BD×(2)C36–C37	20.24	LP(1)N8	BD×(2)O3–C33	45.77
BD(2)C43–C45	BD×(2)O 5–C46	16.47	LP(1)N8	BD×(2)N10–C34	42.38
BD(2)C43–C45	BD×(2)C36–C37	19.96	LP(1)N7	BD×(2)O2–C29	46.69
BD(2)C43–C45	BD×(2)C39–C41	20.07	LP(1)N7	BD×(2)N6–C27	53.25

^a E⁽²⁾ in kcal/mol.

5. Conclusions

A new thieno[2,3-*d*]pyrimidine clubbed with a ninhydrin scaffold linked with hydrazone **4** was synthesized from the reaction of either triketoester **1** or ninhydrin **2** with the thienopyrimidine hydrazide **3** under reflux conditions for 4 h. Different structural characterization tools were used to characterize the structure of the target compound. Single crystals suitable for X-ray diffraction analysis were obtained from the recrystallization in DMF/MeOH. The supramolecular structure of the hydrazone **4** was analyzed using Hirshfeld calculations. DFT calculations were used to calculate the electronic properties of **4** and predict the different ED processes which stabilize the molecular structure of the studied compound via electron conjugation.

Supplementary Materials: The following supporting information can be downloaded at: <https://www.mdpi.com/article/10.3390/cryst13030384/s1>, X-Ray structure determinations; Figure S1: ¹H NMR of compound **4**; Figure S2: ¹³C NMR of compound **4**; Table S1: The calculated geometric parameters of **4**^a.

Author Contributions: Conceptualization, A.B., M.S. and A.T.A.B.; methodology, M.S.A. and M.S.; software, M.H. and S.M.S.; formal analysis, M.S.A. and A.T.A.B.; X-ray crystal structure: M.H.; investigation, M.S.A. and M.S.; resources, A.T.A.B., A.B. and M.S.A.; writing—original draft preparation, A.T.A.B., S.M.S. and A.B.; writing—review and editing A.T.A.B., S.M.S. and A.B.; All authors have read and agreed to the published version of the manuscript.

Funding: Princess Nourah bint Abdulrahman University Researchers Supporting Project number (PNURSP2023R86), Princess Nourah bint Abdulrahman University, Riyadh, Saudi Arabia.

Data Availability Statement: Not applicable.

Acknowledgments: Princess Nourah bint Abdulrahman University Researchers Supporting Project number (PNURSP2023R86), Princess Nourah bint Abdulrahman University, Riyadh, Saudi Arabia.

Conflicts of Interest: The authors declare no conflict of interest.

References

1. Ali, E.M.; Abdel-Maksoud, M.S.; Oh, C.H. Thieno [2,3-*d*] pyrimidine as a promising scaffold in medicinal chemistry: Recent advances. *Bioorg. Med. Chem.* **2019**, *27*, 1159–1194. [[CrossRef](#)] [[PubMed](#)]
2. Bánhegyi, P.; Kéri, G.; Örfi, L.; Szekélyhidi, Z.; Wázquez, F.; Kft, V.C.K. Tricyclic Benzo [4, 5]thieno-[2, 3-*d*] Pyrimidine-4-yl-amin Derivatives, Their Salts, Process for Producing the Compounds and Their Pharmaceutical Use. U.S. Patent 8,802,849, 12 August 2014.
3. Rheault, T.R.; Caferro, T.R.; Dickerson, S.H.; Donaldson, K.H.; Gaul, M.D.; Goetz, A.S.; Mullin, R.J.; McDonald, O.B.; Petrov, K.G.; Rusnak, D.W.; et al. Thienopyrimidine-based dual EGFR/ErbB-2 inhibitors. *Bioorg. Med. Chem. Lett.* **2009**, *19*, 817–820. [[CrossRef](#)] [[PubMed](#)]
4. Wu, C.-H.; Coumar, M.S.; Chu, C.-Y.; Lin, W.-H.; Chen, Y.-R.; Chen, C.-T.; Shiao, H.-Y.; Rafi, S.; Wang, S.-Y.; Hsu, H.; et al. Design and Synthesis of Tetrahydropyridothieno [2,3-*d*]pyrimidine Scaffold Based Epidermal Growth Factor Receptor (EGFR) Kinase Inhibitors: The Role of Side Chain Chirality and Michael Acceptor Group for Maximal Potency. *J. Med. Chem.* **2010**, *53*, 7316–7326. [[CrossRef](#)] [[PubMed](#)]
5. Dai, Y.; Guo, Y.; Frey, R.R.; Ji, Z.; Curtin, M.L.; Ahmed, A.A.; Albert, D.H.; Arnold, L.; Arries, S.S.; Barlozzari, T.; et al. Thienopyrimidine Ureas as Novel and Potent Multitargeted Receptor Tyrosine Kinase Inhibitors. *J. Med. Chem.* **2005**, *48*, 6066–6083. [[CrossRef](#)] [[PubMed](#)]
6. Ameen, M.A.; Ahmed, E.K.; Mahmoud, H.I.; Ramadan, M. Synthesis and screening of phosphodiesterase 5 inhibitory activity of fused and isolated triazoles based on thieno [2, 3-*d*] pyrimidines. *J. Heterocycl. Chem.* **2019**, *56*, 1831–1838. [[CrossRef](#)]
7. Rizk, O.H.; Shaaban, O.G.; El-Ashmawy, I.M. Design, synthesis and biological evaluation of some novel thienopyrimidines and fused thienopyrimidines as anti-inflammatory agents. *Eur. J. Med. Chem.* **2012**, *55*, 85–93. [[CrossRef](#)] [[PubMed](#)]
8. Ameen, M.A.; Ahmed, E.K.; Abdellatifa, F.F. A Novel Synthetic Routes to New 3-Substituted 4-oxo-3,4,5,6,7,8-hexahydropyrido[4,4,5] thieno[2,3]pyrimidine-7-carboxylic Acid Ethyl Ester Derivatives. *Phosphorus Sulfur Silicon Relat. Elem.* **2005**, *180*, 95–107. [[CrossRef](#)]
9. Alagarsamy, V.; Meena, S.; Ramsesh, K.V.; Solomon, V.R.; Thirumurugan, D.K.; Dhanabala, K.; Murugana, M. Synthesis, analgesic, anti-inflammatory, ulcerogenic index and antibacterial activities of novel 2-methylthio-3-substituted-5,6,7,8 tetrahydro benzo(b) thieno [2,3-*d*]pyrimidin-4(3H)-ones. *Eur. J. Med. Chem.* **2006**, *41*, 1293–1300. [[CrossRef](#)]
10. Al-Taisan, K.M.; Al-Hazimi, H.M.; Al-Shihry, S.S. Synthesis, characterization and biological studies of some novel thieno [2,3-*d*]pyrimidines. *Molecules* **2010**, *15*, 3932–3957. [[CrossRef](#)]
11. Ghoraba, M.M.; Osman, A.N.; Noamanc, E.; Heibaa, H.I.; Zahera, N.H. The synthesis of some new sulfur heterocyclic compounds as potential radioprotective and anticancer agents. *Phosphorus Sulfur Silicon Relat. Elem.* **2006**, *181*, 1935–1950. [[CrossRef](#)]
12. Azaba, M.E. Utility of the enamino nitrile moiety in the synthesis of some biologically active thienopyrimidine derivatives. *Phosphorus Sulfur Silicon Relat. Elem.* **2006**, *183*, 1766–1782. [[CrossRef](#)]
13. Abdelrahman, S.; El-Gohary, N.S.; Elbendary, E.; El-Ashry, S.M.; Shaaban, M.I. Synthesis, antimicrobial, antitumor-sensing, antitumor and cytotoxic activities of new series of cyclopenta(hepta)[b]thiophene and fused cyclohepta[b]thiophene analogs. *Eur. J. Med. Chem.* **2017**, *140*, 200–211. [[CrossRef](#)]
14. Lagardère, P.; Fersing, C.; Masurier, N.; Lisowski, V. Thienopyrimidine: A Promising Scaffold to Access Anti-Infective Agents. *Pharmaceuticals* **2022**, *15*, 35. [[CrossRef](#)]
15. Chaykovsky, M.; Lin, M.; Rosowsky, A.; Modest, E.J. 2,4-Diaminothieno [2,3-*d*]pyrimidines as antifolates and antimalarials. 2. Synthesis of 2,4-diaminopyrido [4',3':4,5]thieno [2,3-*d*]pyrimidines and 2,4-diamino-8H-thiopyrano [4',3':4,5]thieno [2,3-*d*]pyrimidines. *J. Med. Chem.* **1973**, *16*, 188–191. [[CrossRef](#)]
16. Gad, E.M.; Nafie, M.S.; Eltamany, E.H.; Hammad, M.S.; Barakat, A.; Boraie, A.T. Discovery of new apoptosis-inducing agents for breast cancer based on ethyl 2-amino-4,5,6,7-tetrahydrobenzo[b] thiophene-3-carboxylate: Synthesis, in vitro, and in vivo activity evaluation. *Molecules* **2020**, *25*, 2523. [[CrossRef](#)]
17. Elmenier, F.M.; Lasheen, D.S.; Abouzid, K.A. Design, synthesis, and biological evaluation of new thieno [2, 3-*d*] pyrimidine derivatives as targeted therapy for PI3K with molecular modelling study. *J. Enzym. Inhib. Med. Chem.* **2022**, *37*, 315–332. [[CrossRef](#)]
18. Laporte, G.M.; Ramotowski, R.S. The effects of latent print processing on questioned documents produced by office machine systems utilizing inkjet technology and toner. *J. Forensic Sci.* **2003**, *48*, 658–663. [[CrossRef](#)]
19. Schwarz, L.; Frerichs, I. Advanced solvent-free application of ninhydrin for detection of latent fingerprints on thermal paper and other surfaces. *J. Forensic Sci.* **2002**, *47*, 1274–1277. [[CrossRef](#)]
20. Petraco, N.D.; Proni, G.; Jackiw, J.J.; Sapse, A.M. Amino acid alanine reactivity with the fingerprint reagent ninhydrin. A detailed ab initio computational study. *J. Forensic Sci.* **2006**, *51*, 1267–1275. [[CrossRef](#)]
21. Alvarez, M.R.; Laiño, R.B.; Díaz-García, M.E. Insights into the ninhydrin chemiluminescent reaction and its potential for micromolar determination of human serum albumin. *J. Lumin.* **2006**, *118*, 193–198. [[CrossRef](#)]
22. Das, S.; Maity, S.; Ghosh, P.; Paul, B.K.; Dutta, A. Base Promoted Tandem Cyclization of o-Phenylenediamine with Ninhydrin-phenol Adducts: An Unprecedented Route to Phenol Appended Isoindolo [2, 1-a] quinoxaline Fluorophore. *ChemistrySelect* **2019**, *4*, 2656–2662. [[CrossRef](#)]
23. Patil, S.A.; Patil, R.; Patil, S.A. Recent developments in biological activities of indanones. *Eur. J. Med. Chem.* **2017**, *138*, 182–198. [[CrossRef](#)] [[PubMed](#)]

24. Verma, G.; Marella, A.; Shaquiquzzaman, M.; Akhtar, M.; Ali, M.R.; Alam, M.M. A review exploring biological activities of hydrazones. *J. Pharm. Bioallied. Sci.* **2014**, *6*, 69–80. [PubMed]
25. Shakdofa, M.; Shtaiwi, M.; Morsy, N.M.; Abdel-Rassel, T.M.A. Metal complexes of hydrazones and their biological, analytical and catalytic applications: A review. *Main Group Chem.* **2014**, *13*, 187–218. [CrossRef]
26. Sharma, A.; Mehta, T.; Shah, M.K. Synthesis and spectral studies of transition metal complexes supported by NO-bidentate Schiff-Base ligand. *Der Chem. Sin.* **2013**, *4*, 141–146.
27. Boraei, A.T.A.; Soliman, S.M.; Haukka, M.; Salama, E.E.; Sopaih, M.; Barakat, A.; Sarhan, A.M. Straightforward green synthesis of indeno-furan carboxylates from ninhydrin and β -ketoesters: X-Ray crystal structure, Hirshfeld and DFT investigations. *J. Mol. Str.* **2022**, *1255*, 132433. [CrossRef]
28. Rikagu Oxford Diffraction. *CrysAlisPro*; Rikagu Oxford Diffraction Inc.: Yarnton, UK, 2022.
29. Sheldrick, G.M. *SADABS—Bruker Nonius Scaling and Absorption Correction*; Bruker AXS, Inc.: Madison, WI, USA, 2012.
30. Sheldrick, G.M. SHELXT-Integrated Space-Group and Crystal-Structure Determination. *Acta Crystallogr. Sect. A Found. Adv.* **2015**, *71*, 3–8. [CrossRef]
31. Hübschle, C.B.; Sheldrick, G.M.; Dittrich, B. *ShelXle*: A Qt graphical user interface for SHELXL. *J. Appl. Crystallogr.* **2011**, *44*, 1281–1284. [CrossRef]
32. Turner, M.J.; McKinnon, J.J.; Wolff, S.K.; Grimwood, D.J.; Spackman, P.R.; Jayatilaka, D.; Spackman, M.A. *Crystal Explorer17*; University of Western Australia: Perth, Australia, 2017; Available online: <http://hirshfeldsurface.net> (accessed on 20 July 2017).
33. Frisch, M.J.; Trucks, G.W.; Schlegel, H.B.; Scuseria, G.E.; Robb, M.A.; Cheeseman, J.R.; Scalmani, G.; Barone, V.; Mennucci, B.; Petersson, G.A.; et al. *GAUSSIAN 09*; Revision A02; Gaussian Inc.: Wallingford, CT, USA, 2009.
34. Dennington, R., II; Keith, T.; Millam, J. (Eds.) *GaussView*; Version 4.1; Semichem Inc.: Shawnee Mission, KS, USA, 2007.
35. Reed, A.E.; Curtiss, L.A.; Weinhold, F. Intermolecular interactions from a natural bond orbital, donor-acceptor viewpoint. *Chem. Rev.* **1988**, *88*, 899–926. [CrossRef]
36. Becke, A.D. Density-Functional Thermochemistry. III. The Role of Exact Exchange. *J. Chem. Phys.* **1993**, *98*, 5648–5652. [CrossRef]
37. Lee, C.; Yang, W.; Parr, R.G. Development of the Colle-Salvetti correlation-energy formula into a functional of the electron density. *Phys. Rev. B* **1988**, *37*, 785–789. [CrossRef]
38. Stephens, P.J.; Devlin, F.J.; Chabalowski, C.F.; Frisch, M.J. Ab Initio Calculation of Vibrational Absorption and Circular Dichroism Spectra Using Density Functional Force Fields. *J. Phys. Chem.* **1994**, *98*, 11623–11627. [CrossRef]
39. Foresman, J.B.; Frisch, A.E. *Exploring Chemistry with Electronic Structure Methods*, 2nd ed.; Gaussian: Pittsburgh, PA, USA, 1996.
40. Chang, R. *Chemistry*, 7th ed.; McGraw-Hill: New York, NY, USA, 2001.
41. Kosar, B.; Albayrak, C. Spectroscopic investigations and quantum chemical computational study of (E)-4-methoxy-2-[(p-tolylimino) methyl] phenol. *Spectrochim. Acta* **2011**, *78*, 160–167. [CrossRef]
42. Koopmans, T.A. Ordering of wave functions and eigenenergies to the individual electrons of an atom. *Physica* **1933**, *1*, 104–113. [CrossRef]
43. Parr, R.G.; Yang, W. *Density-Functional Theory of Atoms and Molecules*; Oxford University Press: New York, NY, USA, 1989.
44. Parr, R.G.; Szentpaly, L.V.; Liu, S. Electrophilicity index. *J. Am. Chem. Soc.* **1999**, *121*, 1922–1924. [CrossRef]
45. Singh, R.N.; Kumar, A.; Tiwari, R.K.; Rawat, P.; Gupta, V.P. A combined experimental and quantum chemical (DFT and AIM) study on molecular structure, spectroscopic properties, NBO and multiple interaction analysis in a novel ethyl 4-[2-(carbamoyl) hydrazinylidene]-3, 5-dimethyl-1H-pyrrole-2-carboxylate and its dimer. *J. Mol. Strut.* **2013**, *1035*, 427–440. [CrossRef]
46. Hubert Joe, I.; Kostova, I.; Ravikumar, C.; Amalanathan, M.; Pinzaru, S.C. Theoretical and vibrational spectral investigation of sodium salt of acenocoumarol. *J. Raman Spectrosc.* **2009**, *40*, 1033–1038.
47. Sebastian, S.; Sundaraganesan, N. The spectroscopic (FT-IR, FT-IR gas phase, FT-Raman and UV) and NBO analysis of 4-Hydroxypiperidine by density functional method. *Spectrochim. Acta Part A Mol. Biomol. Spectrosc.* **2010**, *75*, 941–952. [CrossRef]

Disclaimer/Publisher’s Note: The statements, opinions and data contained in all publications are solely those of the individual author(s) and contributor(s) and not of MDPI and/or the editor(s). MDPI and/or the editor(s) disclaim responsibility for any injury to people or property resulting from any ideas, methods, instructions or products referred to in the content.